TWO-POINT RAY TRACING AND CONTROLLED INITIAL-VALUE RAY TRACING IN 3-D HETEROGENEOUS BLOCK STRUCTURES

Petr Bulant

Department of Geophysics, Charles University, Ke Karlovu 3, 121 16 Praha 2, Czech Republic, E-mail: bulant@seis.karlov.mff.cuni.cz

ABSTRACT

It is well known, that even in quite simple seismic models it is almost never sufficient to perform an initial–value ray tracing on a dense grid followed by interpolation. Alternatively, choosing an arbitrary curve and obtaining a two–point ray by bending is problematic in view of multivaluedness. If the model produces multivalued arrivals, we need some kind of a more advanced two–point ray tracer to find all two–point rays for all the receivers. Different methods are currently being used (e.g. Hanyga 1996, Lucio *et al.* 1996, Vinje *et al.* 1996a, 1996b). Our solution to the two-point ray tracing problem is a sophisticated shooting program, based on an accurate search for the subdomains of ray take-off parameters, where the two–point rays may occur. The subdomains may be found by a special triangularization of the 2-D domain of ray take–off parameters. The two–point rays may be then identified inside triangles whose all three vertices are formed by rays starting in same subdomain and arriving into a receiver area.

Once the domain of ray take-off parameters is triangularized, we can use the triangles mentioned above to construct ray tubes through the model volume, and to interpolate travel times and other quantities inside the tubes, like in the wavefront tracing method (Vinje *et al.* 1993). The described controlled initial–value ray tracing method is a useful extension of two–point ray tracing programs based on triangularization, and it may be very easily applied, once the domain of ray take-off parameters is appropriately triangularized. It allows accurate interpolation of wavefield attributes, e.g. ray–theory travel times, amplitudes and other quantities, at dense grids located in the seismic model. This might be of interest for, e.g., 3-D travel time tomography or ray-theory amplitude migration.

Journal of Seismic Exploration, **8** (1999), 57–75.

INTRODUCTION

The *shooting method* for solving a two-point ray tracing problem is based on iterative application of an *initial–value ray tracing* algorithm. The existing version of the shooting algorithm (Bulant 1996) was designed for two–point ray tracing in considerably general 3-D models of heterogeneous geological structures. In each computation, only the rays of a single *elementary wave*, i.e. the rays whose behavior at structural interfaces is prescribed by an a priori chosen *ray code*, are considered. The rays are thus specified uniquely by the *ray take–off parameters*, e.g. shooting angles in case of a point source. For each given ray code, the described shooting method rests on a sufficiently accurate determination of the boundaries between rays with different *ray histories*, i.e. passing through different geological blocks, across different structural interfaces, terminated in different areas for different reasons, or passing through a different number of caustics. The concept of ray history thus adds more detailed information to distinguish the rays of the selected ray code. The demarcation belts between the different ray histories, corresponding to the numerical uncertainty of the boundaries between the ray histories, have to be kept reasonably narrow, because all two–point rays, situated inside the demarcation belts, will be lost. Once the 2-D domain of ray take–off parameters, the *ray domain,* is decomposed with given accuracy into *homogeneous subdomains*, corresponding to rays of equal ray histories, the two–point rays can be found (e.g. by using the paraxial ray approximation) within the individual homogeneous subdomains of *successful rays* (rays passing through the *reference surface* at which the receivers are situated).

The two–point ray tracing algorithm was described in detail by Bulant (1996). The corresponding Fortran 77 computer code for 3-D two–point ray tracing was developed on the basis of the package `MODEL` to specify block models of geological structures, and the package `CRT` for initial–value ray tracing in the models (Červený *et al.* 1988).

In this paper we shall briefly review the most important steps of the two–point ray tracing algorithm, and discuss how it connects with the controlled initial–value ray tracing algorithm. We shall discuss the problem of the appropriate triangularization of homogeneous subdomains, because it is very important throughout the controlled initial–value ray tracing method. Finally, two numerical examples of the two–point ray tracing are given to show the complexity of the triangularization of the domain of ray take–off parameters. A rough comparison of the presented two–point ray tracing method with dense initial–value ray tracing is given in the conclusions, and principal differences between the described controlled initial–value ray tracing method and the wavefront tracing method (Vinje *et al.* 1993, 1996a, 1996b) are mentioned.

THE TWO–POINT RAY TRACING ALGORITHM

As mentioned above, the principal problem of two–point ray tracing in heterogeneous block models consists in an accurate decomposition of the 2-D ray domain into homogeneous subdomains, corresponding to rays of equal ray histories. In the two–point ray tracing algorithm being described, this decomposition is done by means of sophisticated triangularization of the domain.

A *triangle* in the ray domain is created by three rays. A *basic triangle* is an approximately equilateral triangle with respect to a given metric, the length of its side being given. The apexes of the basic triangle are formed by *basic rays.* A *homogeneous triangle* is a triangle whose apexes are formed by rays with the same ray history.

The ray domain is covered gradually by basic triangles. Basic triangles serve for the initial estimation of the distribution of homogeneous subdomains in the ray domain as well as for choosing the "working area" where the rays are to be held in the computer memory.

When a new basic triangle is created, the next step is to determine whether it is homogeneous. If it is not, it is necessary to divide this new inhomogeneous basic triangle into homogeneous triangles. The method of dividing basic triangles into homogeneous triangles is illustrated in Figures 1 to 4, and explained in this Section.

Note that Figures 1 to 8 are based on two–point ray tracing in the model with lenticular inclusion, described in the numerical examples (see Figure 12). The computation was performed for a point source and a refracted wave, the two histories displayed in Figures 1 to 8 correspond to the rays refracted along the lens and through the lens. Axes in diagrams are plotted without units, because the method is independent of the initial conditions for rays. Ray take–off parameters are normalized and the program works with two normalized ray parameters, both ranging from 0 to 1. Thus, e.g., the rays leaving a point source parametrized by two shooting angles are dealt with in the same way as, e.g., rays from an edge diffractor parametrized by length along the edge and one shooting angle.

First, *boundary rays* on the sides of the triangle have to be found. (The boundary rays are pairs of rays with slightly different ray parameters and different ray histories. Their maximal distance in the ray domain is given a priori. The pairs of boundary rays serve to separate the homogeneous subdomains.) The boundary rays are sought using the method of halving intervals. In each step of this method a new ray i is traced between the two rays j and k of different history. This new ray i together with that one (or both) of rays j,k whose ray history differs from that of ray i is taken to form a new pair, prepared for a next step of halving intervals. This is continued until the distance between the rays, measured in the ray domain, is smaller than the given limit, and the rays are then considered as boundary rays. See Figures 1 and 2. Note that one side of a basic triangle may have several pairs of boundary rays.

The apexes of the triangle together with the boundary rays on its sides are understood to form an *inhomogeneous polygon* from which areas with a uniform ray history, *homogeneous polygons*, are gradually separated. First, any apex of the inhomogeneous polygon is taken to initiate the homogeneous polygon, together with all its other neighboring apexes with the same ray history. The boundary between the subdomain of this ray history and those of other histories is then traced by pairs of boundary rays in order to complete the homogeneous polygon (for details refer to Bulant 1996). See Figure 3.

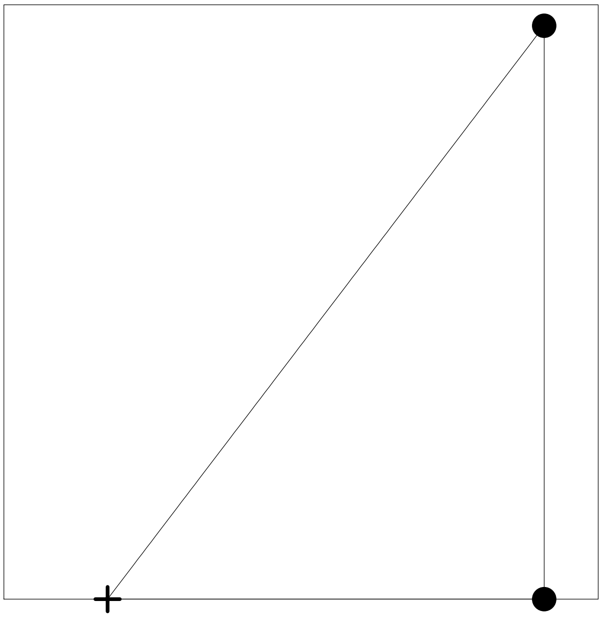

Fig. 1. An inhomogeneous basic triangle in the ray domain is formed by basic rays of different ray histories. Basic rays are symbol–coded according to their history, and they are plotted as larger symbols. The triangle has to be divided into homogeneous triangles to enable further identification of two–point rays within the homogeneous triangles formed by successful rays.

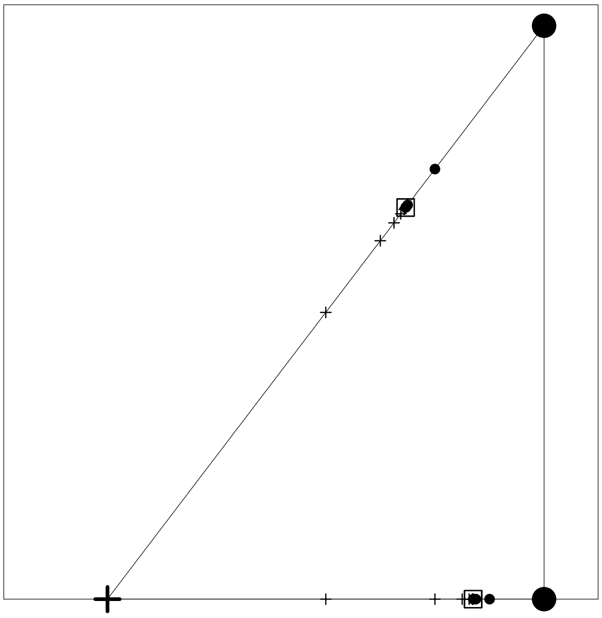

Fig. 2. Searching for boundary rays on the sides of the inhomogeneous triangle by halving intervals. Boundary rays are two rays of different ray history, which are very close each other on the ray domain. Auxiliary rays are plotted as smaller symbols according to their history, and boundary rays are plotted as boxes. Note that the distance between the two boundary rays in each pair is so small that only one box mark can be distinguished.

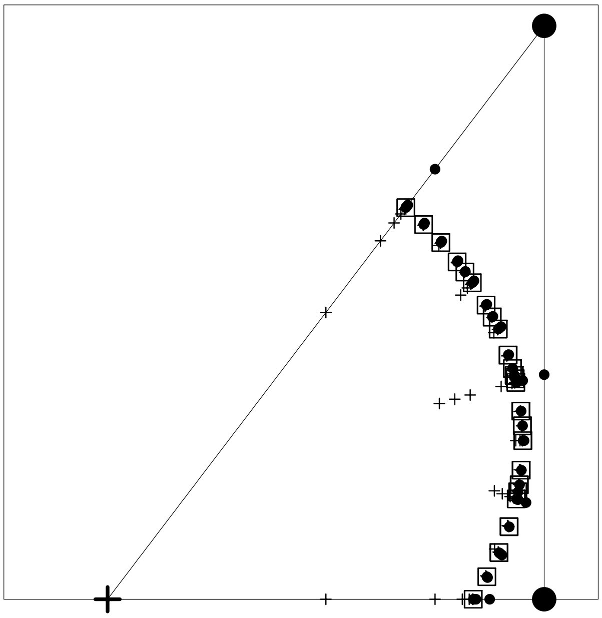

Fig. 3. The boundary between the two ray histories is demarcated by pairs of boundary rays. All the boundary rays of the same ray history together with the basic ray(s) create a homogeneous polygon. There are two homogeneous polygons, which will be covered by homogeneous triangles in the next step.

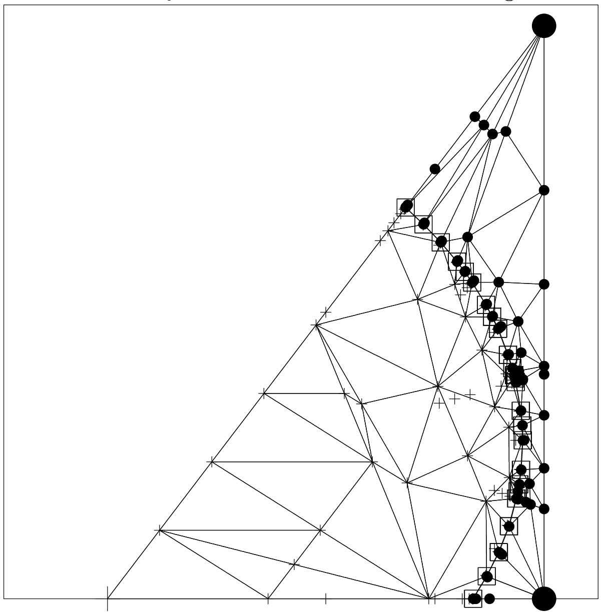

Fig. 4. Both homogeneous polygons are covered by homogeneous triangles. Each homogeneous triangle is formed by three rays of the same ray history. This allows for creation of the ray tube formed by the three rays, for further interpolation within the tube, and for estimation of ray parameters of two–point rays to the receivers located within the reference surface projection of the triangle, if any.

Finally, the homogeneous polygon is covered by homogeneous triangles - Figure 4.

The last step of the solution loop of the two-point ray tracing is a search for two-point rays inside homogeneous *surface triangles*, formed by the points of intersection of the rays with the reference surface. The ray which arrives closest to the receiver on the reference surface is selected, and its distance from the receiver at the reference surface is projected to the ray domain using the paraxial ray approximation. Parameters of a new ray are thus obtained in the ray domain, and the new ray is computed. If the new ray arrives closer to the receiver on the reference surface, it becomes a point of departure for proposing a new ray. This procedure is continued until a ray which is incident sufficiently close to the receiver is found. This ray is then designated as the two-point ray.

If the new ray does not arrive closer to the receiver, the search for the two–point ray is initialized from the ray, which is the second closest to the receiver on the reference surface, if any, and so on. Note that sometimes the procedure need not converge, because the two–point ray need not exist, see Figures 5b, 6b, 7b.

If there is a ray of different history identified in the homogeneous triangle, the ray together with vertices of the triangle is used to create three new inhomogeneous triangles. The algorithm then reverts to the division of these three triangles into homogeneous triangles.

COVERAGE OF THE REFERENCE SURFACE BY SURFACE TRIANGLES

As explained, the final phase of the two–point ray tracing is identifying the two–point rays in the surface triangles. The success of this procedure depends not only on the behavior of the rays, given by the model and by the initial–value ray tracer, but also on the size of the surface triangles and on their distribution on the reference surface. The optimum is regular coverage of the reference surface by approximately equilateral surface triangles of appropriate and approximately the same size.

As mentioned above, the most important part of the two–point ray tracing consists in a very accurate demarcation of the homogeneous subdomains. In each basic triangle the homogeneous subdomains are first represented by homogeneous polygons, which are then covered by homogeneous triangles. This triangularization may be done in different ways. Because of the nonlinear behavior of the mapping from the ray domain to the reference surface, different coverages of the homogeneous polygons in the ray domain produce different shapes of surface triangles, and the arrangement of surface triangles changes dramatically. We shall now demonstrate different coverages of one basic triangle, and show the results obtained, see Figures 5 to 8. We remind the reader, that the figures are based on two–point ray tracing in the model with the lens and that we believe that units are not significant in the presented diagrams.

Firstly, the triangularization depends on whether the tracing of the boundary between the different ray histories takes place in the computation. This strongly affects the whole homogeneous polygon, which is to be covered by homogeneous triangles. See Figures 5 and 6.

The second important effect is connected with the coverage of the homogeneous polygon by homogeneous triangles. The polygon may either be simply divided into triangles (Figure 6), or covered by approximately equilateral triangles (Figure 7). The

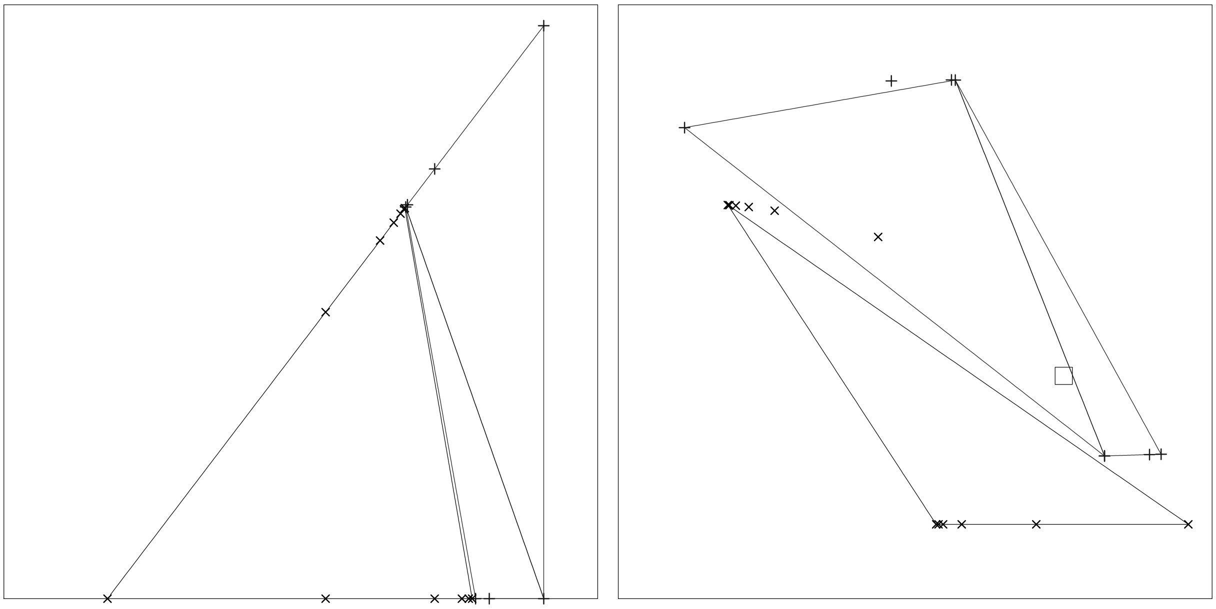

Fig. 5. The simplest version of the shooting algorithm:

(a) An inhomogeneous basic triangle in the ray domain contains successful rays of two different histories. The basic triangle is simply divided into three homogeneous triangles. The boundary between the two ray histories is not traced. Rays are symbol–coded according to their history.

(b) Rays and homogeneous triangles of Figure 5a on the reference surface. A receiver (black box) is situated inside one of the surface triangles of the '+' ray history. The search for the two–point ray to the receiver, which is described at the end of the previous Section, was initialized. However, the two–point ray was not found, because the searching procedure, based on the paraxial ray approximation, did not converge. Why?

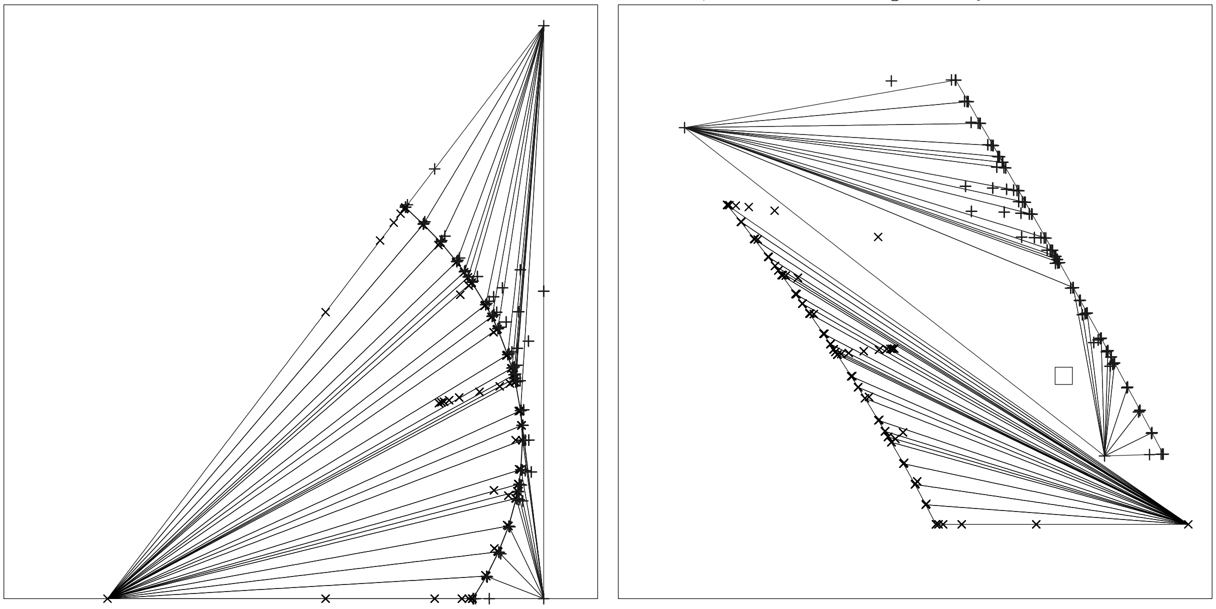

Fig. 6. The first version of shooting algorithm with tracing of the boundary between different ray histories:

(a) The same basic triangle as in Figure 5a. The boundary between the two ray histories is now traced, and the triangle is covered by several thin homogeneous triangles.

(b) Rays and homogeneous triangles of Figure 6a on the reference surface. The two–point ray to the receiver was again not found inside the selected basic triangle, the search for its parameters again did not converge.

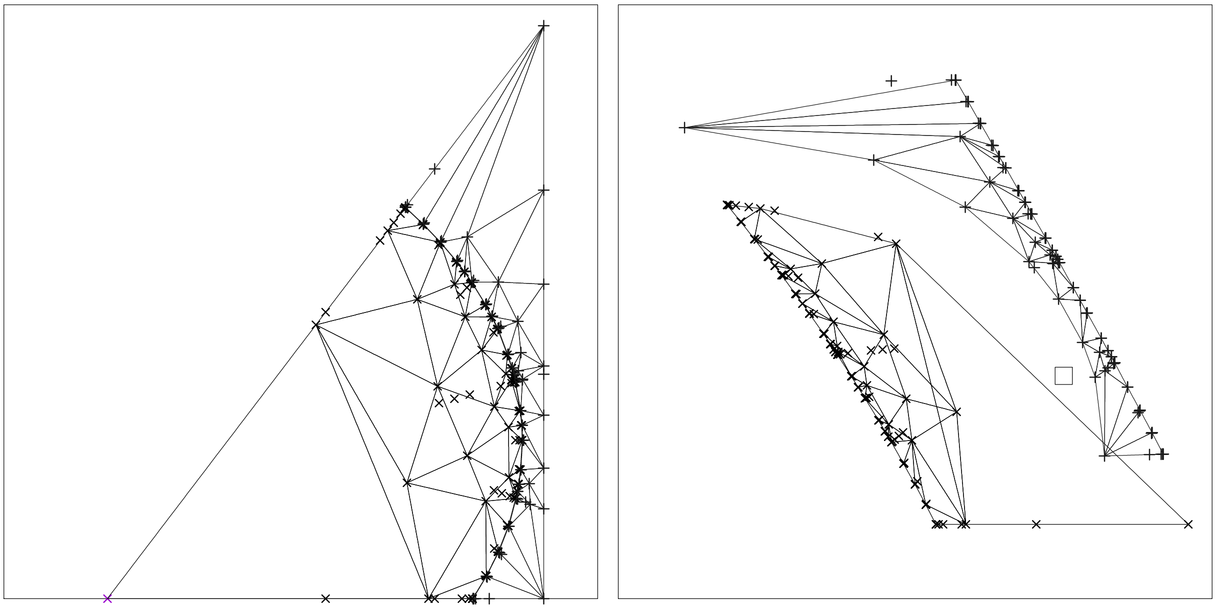

Fig. 7. The version of shooting algorithm with approximately equilateral homogeneous triangles:

(a) Again the same basic triangle as in Figure 5a. The boundary between the two ray histories is now traced, and both subdomains are covered by approximately equilateral homogeneous triangles.

(b) Rays and homogeneous triangles of Figure 7a on the reference surface. The receiver is situated outside the surface triangles. This is the reason why any two–point ray of the '+' history was not found.

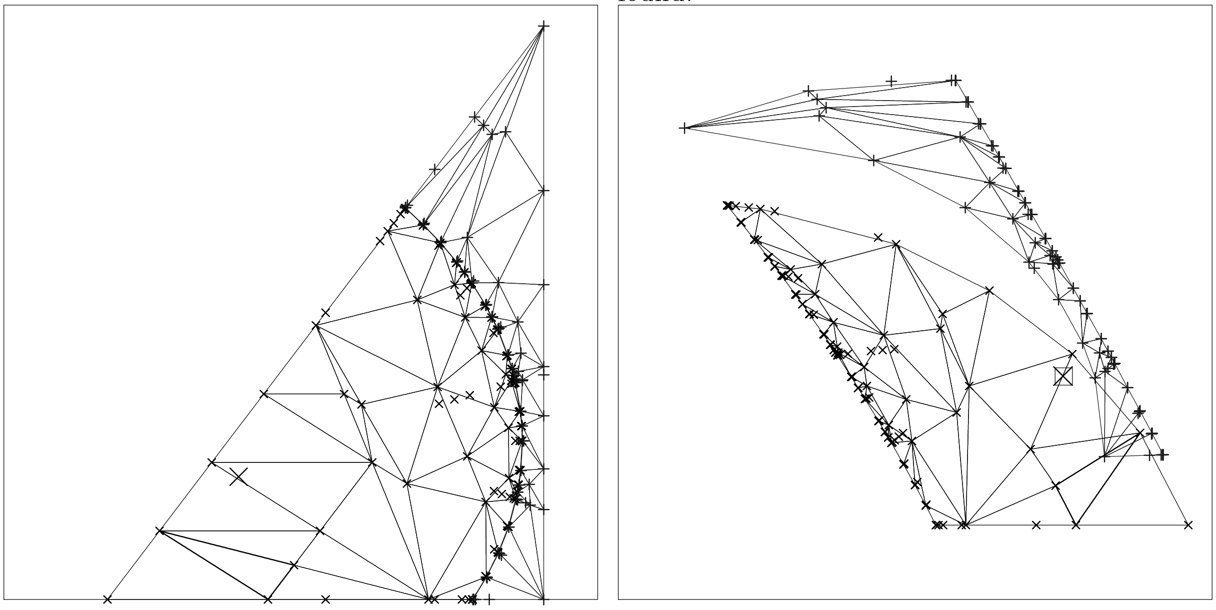

Fig. 8. Current version of the shooting algorithm:

(a) Last time the same basic triangle as in Figure 5a. The boundary between the two ray histories is traced, the triangle is covered by approximately equilateral homogeneous triangles. All the triangles, which are too large on the reference surface, are divided into smaller ones. One two–point ray of the '×' history was identified; it is indicated by a larger symbol.

(b) Rays and homogeneous triangles of Figure 8a on the reference surface. The receiver is situated inside one of the '×' history surface triangles, a two–point ray of the corresponding history was identified. Compare with Figure 5b.

coverage of the polygon by approximately equilateral triangles requires the computation of several new rays, but usually improves the regularity of the surface triangles. This process may even lead to separation of new homogeneous subdomains. Compare Figures 6b and 7b.

The regularity of the surface triangles may be improved by dividing surface triangles which are too large. Each side of every surface triangle that is longer than a chosen parameter is halved, and two new triangles are created. This third difference in covering the homogeneous polygon by homogeneous triangles is demonstrated in Figures 7 and 8.

FROM THE TWO–POINT RAY TRACING ALGORITHM TO THE CONTROLLED INITIAL–VALUE RAY TRACING ALGORITHM

The shooting algorithm, above all based on the procedures of demarcating the boundaries between different ray histories, is thus closely related to *controlled initial–value ray tracing*, whose aim is not to hit given receivers situated at the reference surface, but to cover the model with a sufficiently dense system of rays. The triangularization of homogeneous subdomains corresponding to rays of equal ray histories plays the principal role in controlled initial–value ray tracing. The three rays forming the vertices of a homogeneous triangle are used for construction of a ray tube through the model volume. The spaces between two consecutive wavefronts are then decomposed into *ray cells*, as in the *wavefront tracing method* (Vinje *et al.* 1996a, 1996b), and the travel times and all other calculated quantities may routinely be interpolated within the individual ray cells.

Controlled initial–value ray tracing, which may be viewed as an application of wavefront tracing, is thus a very promising tool for calculation of most energetic ray-theory travel times and amplitudes at gridpoints of dense rectangular grids of points situated in the model volume for, e.g., ray–theory based migration techniques, or the nonlinear determination of seismic hypocentres.

The controlled initial–value ray tracing requires a lot of auxiliary rays to be computed, which are not necessary in wavefront tracing, where they are initiated by interpolation only in case when a ray cell is crossing an interface. On the other hand, in wavefront tracing the rays are traced by parts, which may slow down tracing. New rays are interpolated along a wavefront, which might cause inaccuracy far away from the source. Thus the performance of the final program will probably depend more on the proper and efficient coding than on the selected method.

NUMERICAL EXAMPLES

A three–layer seismic model is used as the first numerical example of using the two–point ray tracing program. The layers are bounded by the plane Earth surface and two curved structural interfaces. The uppermost layer has a constant vertical velocity gradient. The velocity in the middle layer is laterally varying and has a vertical gradient which is higher than the gradient in the uppermost layer. Lateral variations of the velocity are about twice as large as the vertical gradient. The lowermost layer has a constant (and highest) P-wave velocity. The dimensions of the model are approximately 8 x 9.4 x 3 km. The model is based on reflection seismic measurements.

The receivers form a linear profile on the plane Earth surface, where the point source is also situated. Only the rays corresponding to the elementary wave reflected at the lower interface are taken into account in the computation. The model and the computed two–point rays are illustrated in Figure 9.

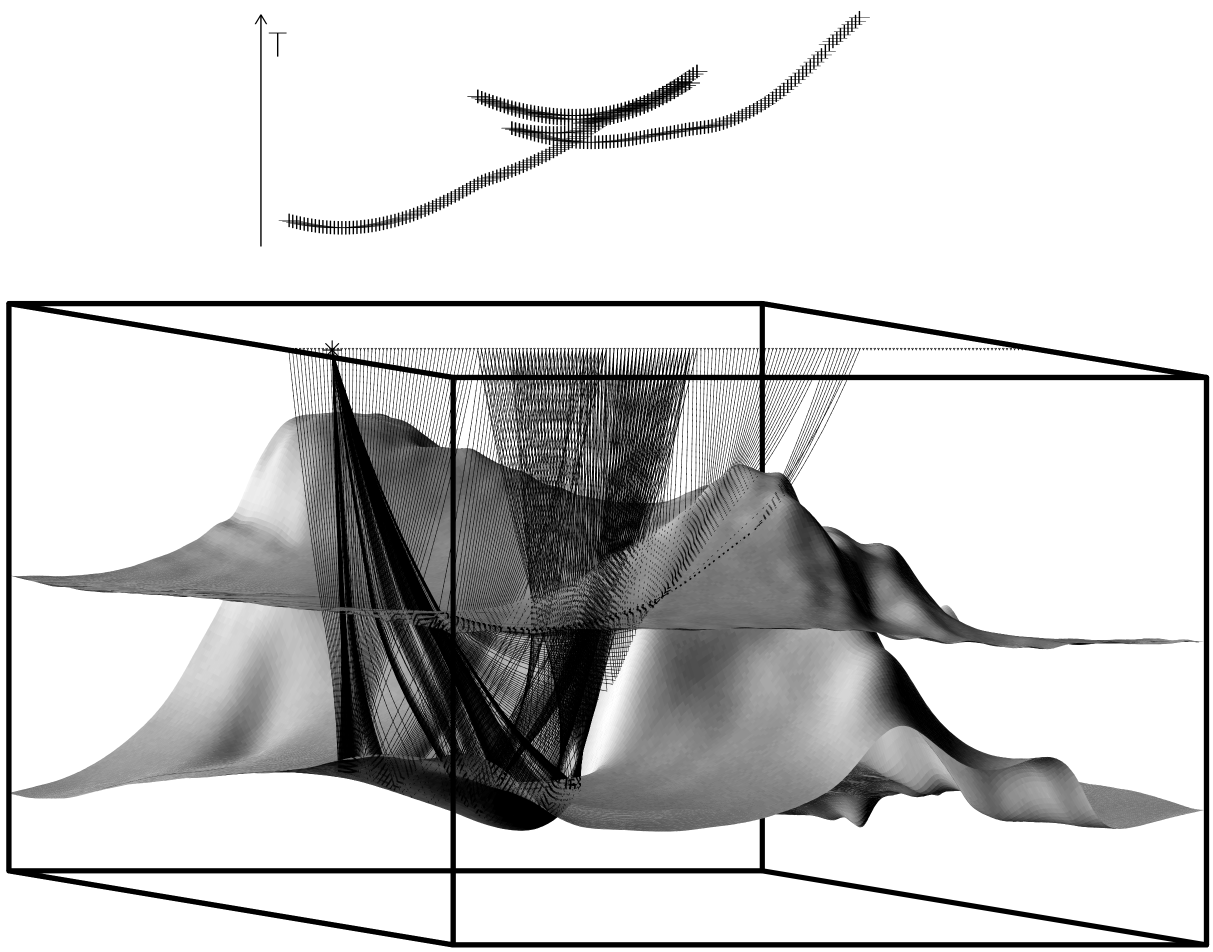

Fig. 9. The three–layer model used as a numerical example of the two–point ray tracing with the two–point rays identified during the computation. The asterisk represents the point source, the small triangles are the receivers. The time curve above the model demonstrates the relative travel times of the two–point rays identified.

The shooting parameters are chosen so that the first parameter corresponds approximately to the angle between the ray and plane xz, and the second to the angle between the ray and plane yz, where x and y are the horizontal axes and z is the vertical axis. The ray domain of the computation in terms of shooting parameters ranges

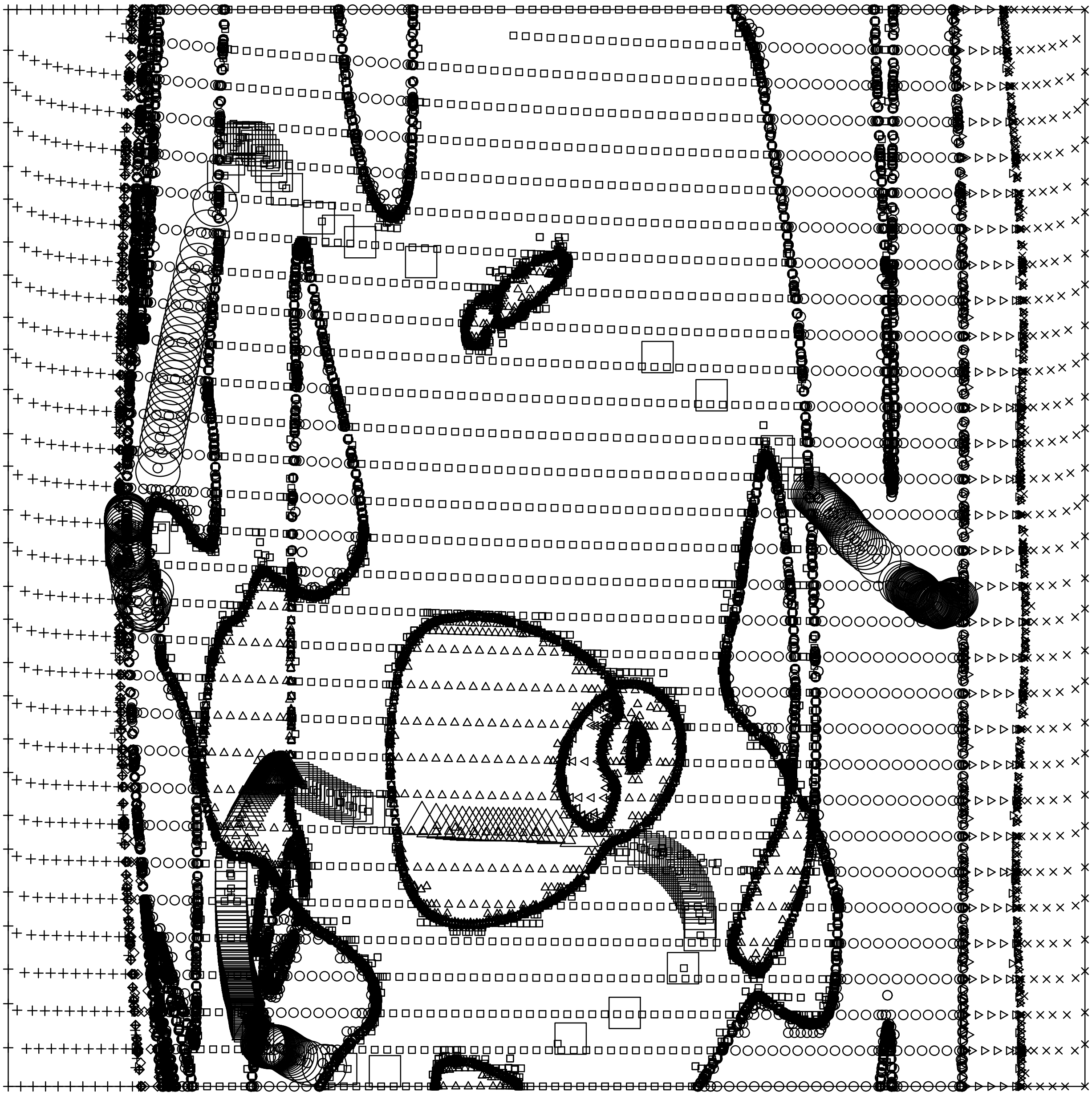

Fig. 10. The coverage of the ray domain by seismic rays shot during the computation. The rays are symbol–coded according to the ray history, two–point rays are plotted as larger symbols. The arrangement of individual homogeneous subdomains is quite complicated. All the subdomains corresponding to successful rays are not connected, because the rays reflect from different parts of the lower interface. The mutual distances between two neighboring two–point rays of the same history provide interesting information about the geometrical spreading inside corresponding homogeneous subdomains.

from -0.05 π to 0.6 π in the direction of the receiver profile, and from -0.17 π to 0.12 π perpendicularly to the profile. 40331 rays with 9 different ray histories are computed and 410 two–point rays are found. The computer time required on a PC Pentium 90 MHz is 1 hour and 5 minutes. Figure 10 displays the coverage of the ray domain by seismic rays. In the figure, we can see several subdomains of successful rays. All of them are not connected, because the rays reflect from different parts of the lower interface. The individual subdomains differ in the ray history according to the number of caustics passed by the rays corresponding to the subdomain.

The maximum length of the sides of the homogeneous triangles on the reference surface (plane Earth surface) is 2 km. The configurations of these homogeneous triangles of individual ray histories on the reference surface are shown in Figure 11. For instance the triangles of the fourth history occupy quite large part of the normalized ray domain (Fig. 10), but very small area on the reference surface. On the other hand the triangles of the second history (circle marks) form several relatively thin and isolated strips on the ray domain, but they cover large area on the reference surface and are folded there.

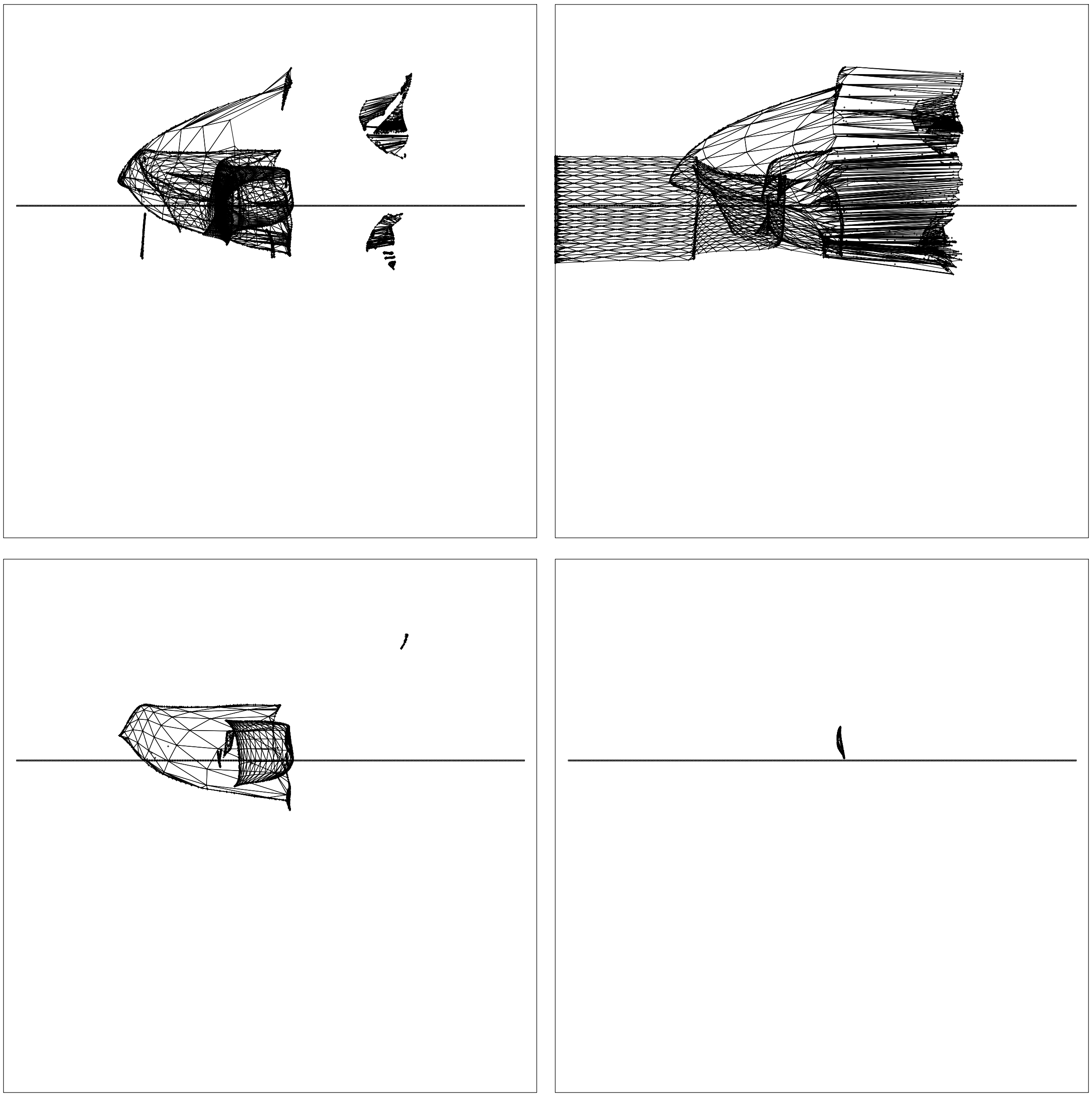

Fig. 11. The coverages of the reference surface by seismic rays and homogeneous triangles of four successful ray histories shot and created during the computation. Many of the triangles are overlapping, which explains the multivaluedness of the travel–time curve shown in the Figure 9. The dimensions of the reference surface are 8 × 9.4 km. The bold black line denotes the receiver profile, the symbol in lower left–hand corner denotes the ray history according to the Figure 10.

The second numerical example of two-point ray tracing in 3-D is the computation of a diffracted elementary wave in a model with a lens. The two-layer model with a smooth curved Earth surface and first–order structural interface has a homogeneous lenticular inclusion in the upper constant velocity gradient layer. The lenticular inclusion has a higher velocity than its neighborhood, and the velocity is highest in the lower layer. The dimensions of the model are: length 60 km, width 40 km, and height 30 km, including the free space. The model is fully artificial, it is the demo model of the MODEL package.

Two-point ray tracing of the elementary wave diffracted at the edge of the lenticular inclusion is performed from the point source, receivers form a linear profile on the curved Earth surface. The computation of the diffracted wave is stepwise.

In the first step, the upper structural interface bounding the lens is understood to be the reference surface, and receivers are placed along the edge (which, of course, lies at the reference surface) with a regular step. Two–point rays are then computed from the point source to the receivers (to the edge). Only the rays corresponding to the refracted elementary wave are taken into account in this numerical example. See Figure 12.

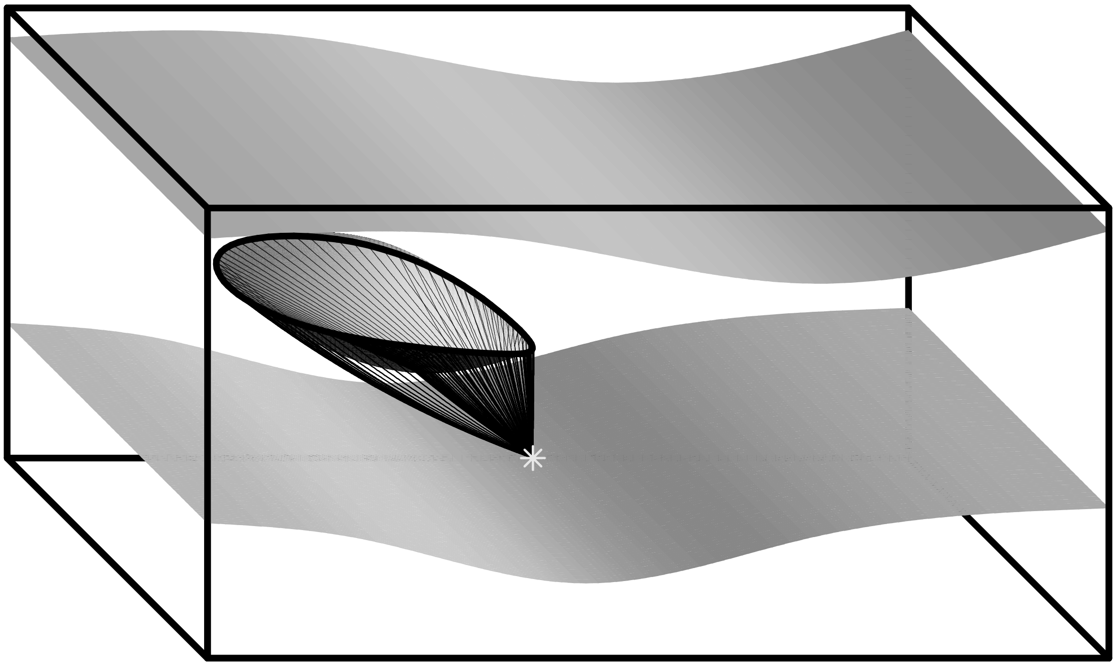

Fig. 12. First step of the computation of diffracted rays in the model with lens. The rays from the point source to the edge of the lenticular inclusion are computed. Only refracted rays are considered. The asterisk represents the point source, the dots are the receivers, placed along the edge. Only the two–point rays identified during the computation are shown in the figure.

The rays of one single history computed in the first step are chosen in the second step. These are rays, which propagated through the lens, but alternatively they might be also the direct rays. The edge diffractor is now understood to be a line source, the initial travel time is interpolated using the travel times of the chosen two–point rays. Note that the ray domain of the line source is again 2-dimensional, the first ray take–off parameter is a length along the edge, and the second is the shooting angle. (For each point on the edge only one shooting angle is free, the second one is given by Snell's law.) One selects the elementary wave to be computed (in the presented example this is the refracted wave), and the two-point rays from the edge to the receiver profile are traced.

See Figure 13. The travel times of the rays leaving the point source, diffracted at the edge, and reaching the receivers are now available.

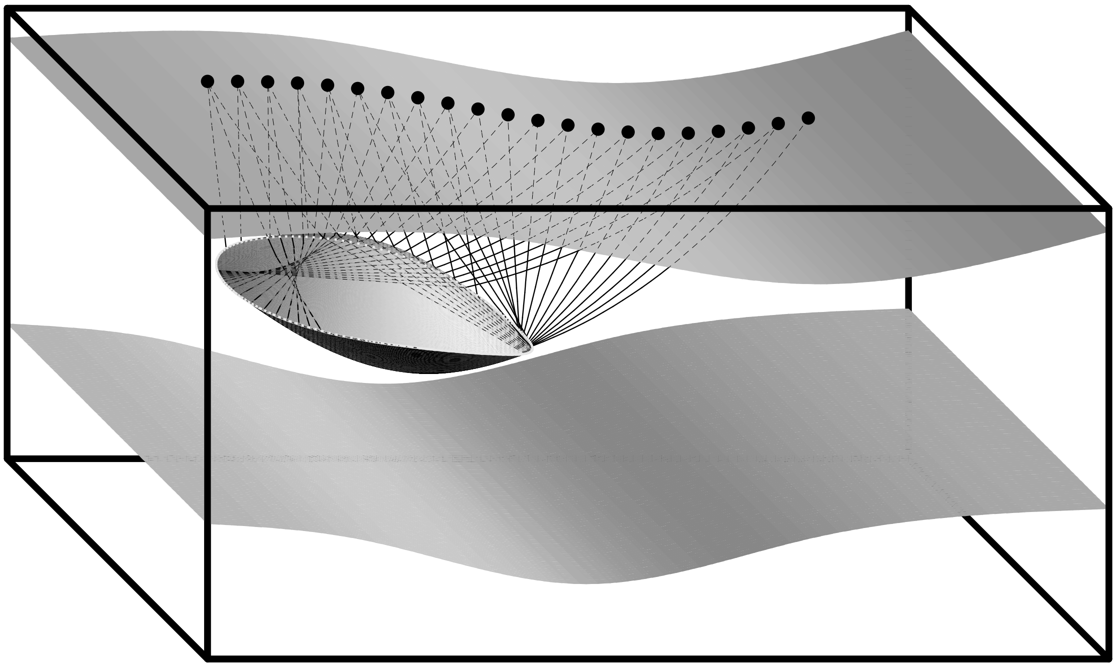

Fig. 13. The second step of the computation of diffracted rays in the model with the lens. The rays from the edge of the lenticular inclusion to the receivers are computed. Only refracted rays are considered. The line represents the edge diffractor, the dots are the receivers. Only the two–point rays identified during the computation are shown in the figure.

The third step (for the purpose of plotting) is similar to the first one. The rays from the point source to the points of departure of the two–point rays, computed in the second step, are traced. Only those rays of the history selected in the second step are taken into account. This results in the final display of the diffracted rays — Figure 14.

CONCLUSIONS

An algorithm for two-point ray tracing in a 3-D heterogeneous medium has been developed. Special emphasis was put on the sufficiently accurate determination of the boundaries between rays with different ray histories, and on finding all the homogeneous subdomains of the ray domain. Consequently, the algorithm is very reliable in computing all two-point rays of the given elementary waves to the given receivers, including multivalued arrivals.

The two-point ray tracing algorithm described is relatively demanding with regard to the number of rays to be traced. The number of rays, which have to be computed, is not significantly affected by the number of receivers, but it is mostly influenced by number of auxiliary rays required to divide the domain of the ray take–off parameters into regions with the same ray history. The method is highly reliable in finding two–point rays in very thin regions of the ray domain. This might be of interest for, e.g., 3-D travel time tomography, or for interpretation and model verification purposes.

In each computation, the width of the demarcation belts is kept below some prescribed limit. This enables to roughly estimate the number of rays which should be

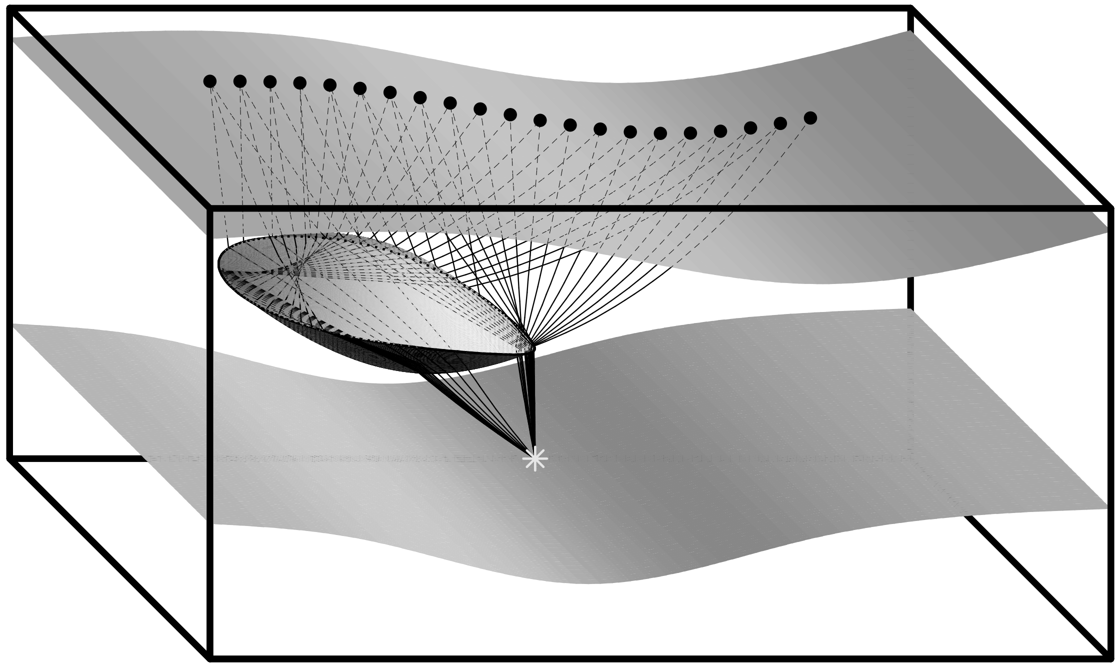

Fig. 14. Final result — the two-point rays leaving the point source, refracted through the lens, diffracted at the edge of the lenticular inclusion, and reaching receivers without reflection at any interface are computed.

traced in initial–value ray tracing on a regular rectangular grid of ray take–off parameters in order to obtain a resolution which is approximately equal to the width of the demarcation belts in the described two–point ray tracing method:
Computation in the three-layer model:

- Dimension of the ray domain: 100×30 units
- Given maximum distance between two rays of different histories forming a pair of boundary rays: 0.002 units
- Regular–grid initial–value ray tracing:
  $(100/0.002) \times (30/0.002) = 50\ 000 \times 15\ 000 = \mathbf{750\ 000\ 000}$ rays
- Shooting program described: **40 331** rays

Appropriate triangularization of homogeneous subdomains is essential for successful solution of the two-point ray tracing problem. It also enables to extend the two-point ray tracing algorithm to the controlled initial-value ray tracing algorithm.

ACKNOWLEDGMENTS

This research has been supported by the consortium "Seismic Waves in Complex 3-D Structures". The author expresses thanks to Dr Luděk Klimeš for his valuable help during the work on the two-point ray tracing routines and to Dr P. M. Bakker for carefully reading the paper.

REFERENCES

Bulant, P. (1996): Two–point ray tracing in 3-D. Pure and Applied Geophysics **148**, 421–447.

Červený, V., Klimeš, L. & Pšenčík, I. (1988): Complete seismic–ray tracing in three–dimensional structures. In: Doornbos, D.J. (ed.), Seismological Algorithms, pp. 89–168. Academic Press, New York.

Hanyga, A. (1996): Point-to-curve ray tracing. Pure and Applied Geophysics **148**, 387–420.

Lucio, P.S., Lambaré, G. & Hanyga, A. (1996): 3D multivalued travel time and amplitude maps, Pure and Applied Geophysics **148**, 449–479.

Vinje, V., Iversen, E. & Gjøystdal, H. (1993): Traveltime and amplitude estimation using wavefront construction. Geophysics, **58**, 1157–1166.

Vinje, V.,Iversen, E., Gjøystdal, H. & Åstebøl, K. (1996a): Estimation of multivalued arrivals in 3D models using wavefront construction – Part I. Geophys. Prospecting, **44**, 819–842.

Vinje, V.,Iversen, E., Gjøystdal, H. & Åstebøl, K. (1996b): Part II: Tracing and interpolation. Geophys. Prospecting, **44**, 843–858.